

Dynamics of Back Electron Transfer in Dye-Sensitized Solar Cells Featuring 4-*tert*-Butyl-Pyridine and Atomic-Layer-Deposited Alumina as Surface Modifiers

Michael J. Katz,[†] Michael J. DeVries Vermeer,^{†,‡} Omar K. Farha,^{†,§} Michael J. Pellin,^{†,‡} and Joseph T. Hupp^{*,†,‡,||}

[†]Department of Chemistry and Argonne-Northwestern Solar Energy Research (ANSER) Center, Northwestern University, 2145 Sheridan Road, Evanston, Illinois 60208, United States

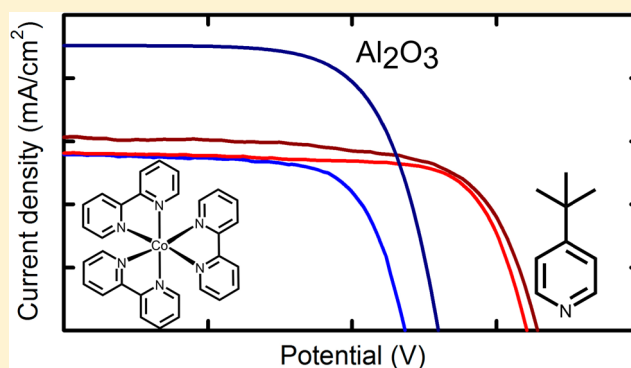
[‡]Materials Science Division, Argonne National Laboratory, 9700 S. Cass Ave., Argonne, Illinois 60439, United States

[§]Department of Chemistry, Faculty of Science, King Abdulaziz University, Jeddah, Saudi Arabia

^{||}Chemical Sciences and Engineering Division, Argonne National Laboratory, 9700 S. Cass Ave., Argonne, Illinois 60439, United States

Supporting Information

ABSTRACT: A series of dye-sensitized solar cells (DSCs) was constructed with TiO₂ nanoparticles and N719 dye. The standard I₃⁻/I⁻ redox shuttle and the Co(1,10-phenanthroline)₃^{3+/2+} shuttle were employed. DSCs were modified with atomic-layered-deposited (ALD) coatings of Al₂O₃ and/or with the surface-adsorbing additive 4-*tert*-butyl-pyridine. Current–voltage data were collected to ascertain the influence of each modification upon the back electron transfer (ET) dynamics of the DSCs. The primary effect of the additives alone or in tandem is to increase the open-circuit voltage. A second is to alter the short-circuit current density, *J*_{SC}. With dependence on the specifics of the system examined, any of a myriad of dynamics-related effects were observed to come into play, in both favorable (efficiency boosting) and unfavorable (efficiency damaging) ways. These effects include modulation of (a) charge-injection yields, (b) rates of interception of injected electrons by redox shuttles, and (c) rates of recombination of injected electrons with holes on surface-bound dyes. In turn, these influence charge-collection lengths, charge-collection yields, and onset potentials for undesired dark current. The microscopic origins of the effects appear to be related mainly to changes in driving force and/or electronic coupling for underlying component redox reactions. Perhaps surprisingly, only a minor role for modifier-induced shifts in conduction-band-edge energy was found. The combination of DSC-efficiency-relevant effects engendered by the modifiers was found to vary substantially as a function of the chemical identity of the redox shuttle employed. While types of modifiers are effective, a challenge going forward will be to construct systems in ways in which the benefits of organic and inorganic modifiers can be exploited in fully additive, or even synergistic, fashion.



1. INTRODUCTION

Energy conversion is initiated in molecular-dye-sensitized solar cells (DSCs) when chromophores bound to high surface area semiconductors are excited via light absorption. Excited electrons are injected into the semiconductor. The oxidized dye molecules are then regenerated by redox shuttles in solution. The injected electrons traverse the semiconductor network to the current collector, move to the external circuit, and ultimately reach the complementary form of the redox shuttle in the cell solution via a dark electrode.^{1–5}

Since the introduction of high-surface-area photoelectrodes in 1991,⁶ and the concomitant Beamon-esque leap⁷ in energy conversion efficiency (from less than 1% to ca. 7%), a great deal of research has gone into both understanding what limits

efficiencies and further improving efficiency. These efforts have included sizable investments in designing and creating new dyes,^{8,9} photoelectrode architectures,¹⁰ redox shuttles,^{11–17} interface modifications,^{18,19} and cell solution compositions.²⁰ Among the largest contributors to efficiency loss in the best-existing manifestations of DSCs are kinetic overpotentials for dye regeneration and for electron injection. For near-champion devices based on ruthenium dyes and the iodide/tri-iodide shuttle and operating at 11+%,²¹ nearly half of the theoretical

Special Issue: John R. Miller and Marshall D. Newton Festschrift

Received: June 18, 2014

Revised: August 14, 2014

Published: August 15, 2014

maximum cell voltage (either the open-circuit photovoltage (V_{oc}) or the voltage at the maximum powerpoint) is lost to these processes.^{21,22} Overpotential-related losses are similarly sizable for recently described dual-sensitizer cells operating at 12+% and utilizing a cobalt-based redox shuttle.⁵

DSCs operate via a series of electron transfer (ET) processes, each of which must compete kinetically against an undesirable back-ET reaction or other process (for example, dye luminescence) that degrades photocurrent production. In a well-designed cell that mitigates against losses due to inefficient photon delivery (e.g., reflection losses, light harvesting, electron injection, dye regeneration, shuttle transport, and counter-electrode turnover of the redox shuttle), the maximum photocurrent density obtainable at short-circuit (J_{SC-max}) is determined by the ground-state/lowest-excited-state energy gap (roughly the HOMO/LUMO gap) of the dye, and the available solar flux at and above the gap.²¹ For the archetypal Ru dye, N719, this is about 18.4 mA/cm² at 1 sun (given a 90% incident-photon-to-current efficiency (IPCE), photon losses of ca. 15% in the visible region due to reflections and due to competitive absorption by the cell solution, and losses of up to 100% in the UV region due to competitive absorption by the current collector, typically a conductive oxide). However, if the dye is not regenerated quickly enough, or if diffusion of the redox shuttle is too slow, then J_{max} is further limited by the slower of these pathways, yielding J'_{max} .²³ To complicate matters, if the injection efficiency (η_{inj}) is not unity then photocurrents are further lowered (to $J'_{max}\eta_{inj}$).

The short-circuit current density (J_{SC}), can thus be written as the forward photocurrent density ($J'_{max}\eta_{inj}$) plus the sum of the current densities due to detrimental (reverse) pathways (J_{det}). The main rate processes contributing to J_{det} are interception of electrochemically or photochemically injected electrons within the semiconductor by the oxidized form of the redox shuttle and back ET from the semiconductor to the oxidized dye. We term the first “electron interception” and the second “charge recombination.” Notably, charge recombination occurs only under illumination; thus, its contributions are undetected by standard dark-current measurements. Equations 1 and 2 delineate how an illuminated cell’s current density is affected by the various competing processes:

$$J = J'_{max}\eta_{inj} + J_{det} \quad (1)$$

$$J_{det} = J_{interception} + J_{recombination} \quad (2)$$

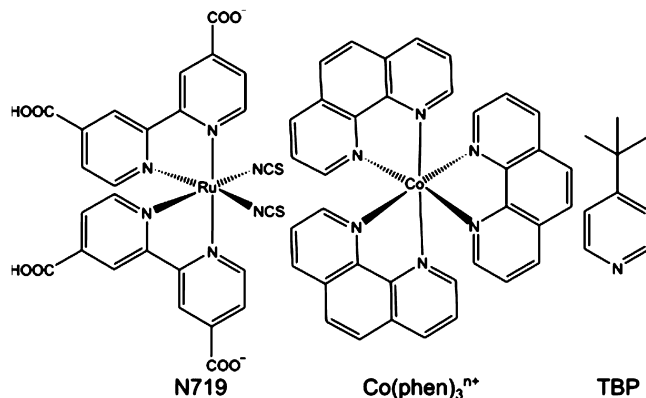
J_{det} which is oppositely signed to J_{max} typically is strongly potential-dependent. The potential at which it precisely offsets J_{SC} ²⁴ defines the DSC open-circuit photovoltage (V_{oc}). Consequently, cell modifications that diminish J_{det} if unaccompanied by compensating effects upon $J'_{max}\eta_{inj}$ will tend to increase V_{oc} , and therefore, the overall DSC energy-conversion efficiency, η .

Given these many processes, and their ability to simultaneously influence J_{SC} , V_{oc} , and fill factors, rational hypothesis-driven advances in DSC performance tend to require an understanding of rate dynamics at the various interfaces.^{25–28} Among the many interesting approaches to rate modification and DSC efficiency enhancement are (a) the addition of 4-*tert*-butyl-pyridine (TBP) to the cell solution (followed by its adsorption at the photoelectrode/solution interface)^{29–33} and (b) the formation of ultrathin coatings of insulating and surface-state-passivating materials such as alumina.^{34–45} The former has been shown to boost values for V_{oc} by up to 340

mV.⁴⁶ The latter is capable, in extreme cases, of increasing V_{oc} by as much as 390 mV,⁴⁷ albeit often with offsetting decreases in photocurrent density. One interpretation of the voltage boosts is that additives (of both kinds) shift the conduction band edge of the photoelectrode in the negative electrochemical direction, thereby engendering equivalent negative shifts in the photoelectrode’s quasi-Fermi level under conditions of open-circuit illumination.^{48–50}

We recently investigated the roles of added TBP and atomic-layer deposited (ALD) alumina in altering specifically the rates and dynamics of electron-interception (i.e., capture of injected electrons by the oxidized form of the redox shuttle). We probed the effects mainly by evaluating dark currents. We observed that both modifiers suppress potential-dependent dark currents, and further, that the suppression effects are roughly additive.⁵¹ To our surprise, however, TBP and ALD alumina were found to influence $J_{interception}$ by mechanisms other than shifts in conduction-band-edge energy (E_{cb}). Indeed, despite anticipated energy contributions from preferential orientation of molecular dipoles and other phenomena,^{48–50} E_{cb} was found to be only slightly changed (a few tens of millivolts or less) by addition of either substance to the electrode/solution interface, as demonstrated by Mott–Schottky measurements of flat-band potentials (E_{fb}).⁵¹

These earlier studies were done with simplified and experimentally idealized systems (i.e., well-defined, ALD-fabricated, flat TiO₂ electrodes) and were limited to dark-current investigations at dye-free interfaces. Here we extend the studies to high-area nanoparticulate photoelectrodes, and we employ the electrodes, with dye coatings and under illumination, in fully assembled cells. We utilize I₃[−]/I[−] and Co(phen)₃^{3+/2+} as redox shuttles (phen = 1,10-phenanthroline). We find that in addition to modulating electron interception, the organic and inorganic surface modifiers alter both charge-injection yields and rates for charge recombination. The importance of the latter, in terms of changes in DSC performance, is found to depend strongly on the chemical identity of the redox shuttle employed.



2. EXPERIMENTAL SECTION

Unless otherwise indicated, all reagents were purchased from commercial sources and used without further purification. Both 8 and 15 Ω cm^{−2} fluorine-doped tin oxide (FTO) glass were purchased from Hartford Glass. [Co(phen)₃](PF₆)₂, [Co(phen)₃](PF₆)₃, (phen = 1,10-phenanthroline) were made according to literature procedures; briefly, Co(NO₃)₂·(H₂O)₆ was dissolved in a minimum amount of methanol. To the reaction mixture was added 3.3 equiv of phen, likewise

dissolved in a minimum amount of methanol. A ca. 10-fold excess of NH_4PF_6 was added to the reaction mixture. The Co shuttle was then precipitated by addition of water. Oxidation of Co(II) to Co(III) was carried out with NOBF_4 in CH_3CN and isolated via the addition of NH_4PF_6 , followed by water.

All electrolyte shuttle solutions were prepared in acetonitrile by mixing 0.02 M of the oxidized form (i.e., Co(III) or I_3^-), 0.2 M of the reduced form (i.e., Co(II) or I^-), and 0.2 M LiClO_4 . In some cells, 0.2 M 4-*tert*-butyl-pyridine was also included.

2.1. Electrode Preparation. Photoanodes were prepared on $8 \Omega \text{ cm}^{-2}$ FTO glass. $1.5 \times 1.5 \text{ cm}$ Squares were cut and then sonicated in water with detergent for 15 min. The samples were rinsed with deionized water and then sonicated in isopropanol for 15 min, followed by methanol for an additional 15 min. After air drying, the electrodes were heated to 500°C for 1 h with the aim of removing organic residues.

Counter electrodes were prepared on $15 \Omega \text{ cm}^{-2}$ FTO glass. $2.0 \times 2.0 \text{ cm}$ Squares, each with one hole drilled, were cleaned in an identical manner to the photoanodes. The clean counter electrodes were evenly coated with $13 \mu\text{L}$ of a 0.5 mM isopropanol solution of H_2PtCl_6 and then placed in an oven at 500°C for 30 min to produce the platinum-coated counter electrode.

A ca. 10 nm blocking layer of TiO_2 was grown on the electrode via atomic layer deposition (Savannah 100 reactor, Cambridge Nanotech, Inc.) using alternating half-cycles of titanium isopropoxide (0.1 s pulse, 1 s exposure, 10 s nitrogen purge) and water (0.1 s pulse, 1 s exposure, 15 s nitrogen purge). Three-hundred full cycles were used. The reactor temperature was maintained at 200°C . The prepared films were then heated at 475°C for 6 h.

TiO_2 nanoparticles (Dyesol) were doctor-bladed onto the electrode through a 0.25 cm^2 hole in a piece of scotch tape. The films were then placed in an oven at 80°C . The tape was removed, and the films were annealed at 450°C over the course of 6 h. The annealed films were ca. $6 \mu\text{m}$ thick.

Alumina-coated TiO_2 films were prepared by ALD-coating the annealed TiO_2 films using 1 cycle of trimethyl aluminum (0.03 s pulse, 1 s exposure, 30 s purge) and deionized water (0.1 s pulse, 1 s exposure, and 30 s purge). One ALD cycle results in formation of roughly one-third of a monolayer of alumina. ALD conditions were chosen to uniformly coat all TiO_2 surfaces of the doctor-bladed nanoparticle films.

Films were dye-soaked overnight in a 0.5 mM ethanolic solution of N719 {Dyesol; N719: $(\text{Bu}_4\text{N})_2[\text{Ru}(\text{dcbp})_2(\text{NCS})_2]$ (dcbp = 4,4'-dicarboxy-2,2'-bipyridine)}. They were subsequently rinsed with ethanol to remove unattached dye.

The photo- and counter-electrode were sandwiched together by melting a $25 \mu\text{m}$ thick piece of Surlyn, having a hole slightly larger than the diameter of the photoanode, between the two electrodes. The edge of the photoanode was sanded and silver epoxy was spread over the edge in order to form a good electrical contact with the FTO.

Electrolyte solution was vacuum backfilled into the cell via capillary forces through a drilled hole in the counter electrode. The hole was then sealed by melting a second piece of Surlyn over the counter electrode.

2.2. Electrochemical Measurements. Photoelectrochemical measurements were carried out with a Solartron "Analytical Modulab" instrument equipped with a 1 MHz frequency analyzer and a potentiostat capable of measuring 1 million samples/second interfaced with a Horiba FluoroLog-3 fluorometer equipped with a 450 W ozone-free xenon lamp.

The fluorometer slit width and sample holder were positioned so as to set light intensity to 100 mW cm^{-2} after passing through an AM1.5 solar filter.

3. RESULTS

3.1. J - V Curves under Illumination. Plots of photo-current-density versus cell voltage (J - V plots) are shown in Figure 1. Independent of surface modifier, values for J_{SC} were

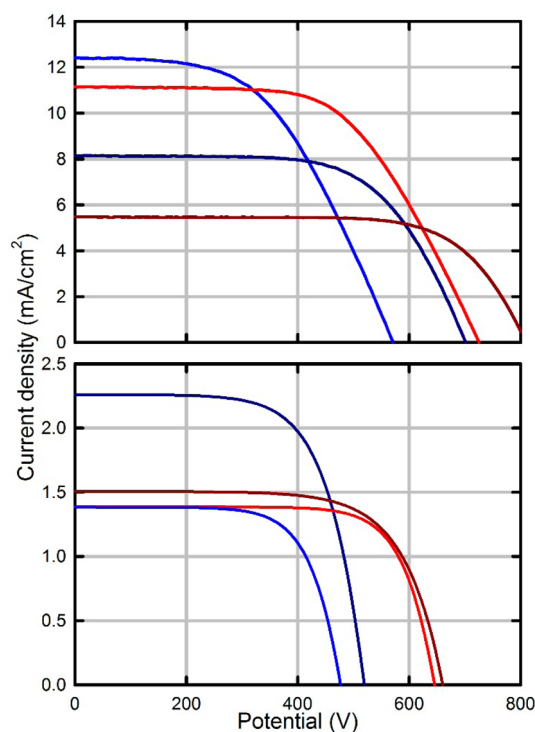


Figure 1. Current vs voltage plots of DSCs containing I_3^-/I^- (top) and $\text{Co}(\text{phen})_3^{3+/2+}$ (bottom). Blue: no modifier; red: TBP; dark blue: Al_2O_3 ; brown: TBP and Al_2O_3 .

lower for cells containing $\text{Co}(\text{phen})_3^{3+/2+}$ than for cells containing I_3^-/I^- . For I_3^-/I^- , J_{SC} decreases in the order of $J_{\text{SC}}(\text{no modifier}) > J_{\text{SC}}(\text{TBP}) > J_{\text{SC}}(\text{Al}_2\text{O}_3) > J_{\text{SC}}(\text{Al}_2\text{O}_3 \text{ and TBP})$; the modifiers only decreased the observed photocurrents. However, for $\text{Co}(\text{phen})_3^{3+/2+}$, ALD alumina boosted J_{SC} by ca. 65%, whereas introduction of TBP had no effect upon J_{SC} . Curiously, the inclusion of both modifiers with $\text{Co}(\text{phen})_3^{3+/2+}$ yielded current that were only 15% higher than the modifier-free devices.

Independent of the redox shuttle employed, open-circuit photovoltages were ordered as follows: $V_{\text{OC}}(\text{no modifier}) < V_{\text{OC}}(\text{Al}_2\text{O}_3) < V_{\text{OC}}(\text{TBP}) < V_{\text{OC}}(\text{Al}_2\text{O}_3 \text{ and TBP})$. The maximum voltage increases (i.e., those obtained by combining modifiers) were ca. 220 mV.

For I_3^-/I^- -containing cells, the overall energy conversion efficiency (η) is largest when just TBP is employed as the modifier. Despite the increased V_{OC} when Al_2O_3 is employed (either alone or in tandem with TBP), the overall efficiency decreases due to decreases in J_{SC} . When $\text{Co}(\text{phen})_3^{3+/2+}$ was used, η was lowest for modifier-free cells. By increasing V_{OC} by ca. 200 mV, TBP increases the overall efficiency. The efficiencies of cells modified with Al_2O_3 are maximal. However, when both Al_2O_3 and TBP are employed, the efficiencies are only slightly higher than devices modified only with TBP; the

increase in V_{OC} in DSCs containing both Al_2O_3 and TBP is offset by the decrease in the J_{SC} relative to the DSCs modified only with Al_2O_3 .

3.2. Dark J - V Curves. Figure 2 shows the dark J - V responses for DSCs containing either I_3^-/I^- or $Co(phen)_3^{3+/2+}$,

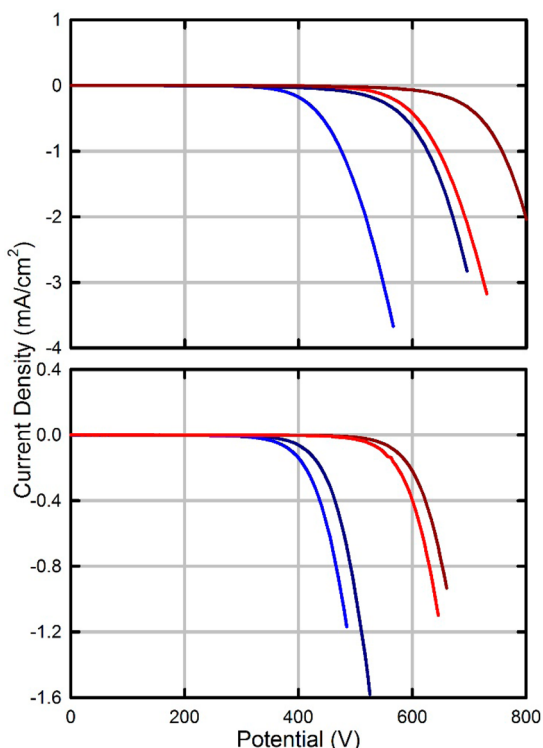


Figure 2. Plots of dark current vs voltage of DSCs containing I_3^-/I^- (top) and $Co(phen)_3^{3+/2+}$ (bottom). Blue: no modifier; red: TBP; dark blue: Al_2O_3 ; brown: TBP and Al_2O_3 .

with and without electrode surface modifiers. The dark currents are plotted out to the value of V_{OC} for the corresponding illuminated systems.⁵² Briefly, for both shuttles, both modifiers serve to suppress dark current (or stated differently, both serve to inhibit shuttle interception of electrochemically injected electrons). When the modifiers are used in tandem, partially additive changes in the potential for onset of dark current are observed. Clearly, suppression of dark current provides a reasonable qualitative accounting of the effects of modifiers upon open-circuit photovoltages (although, as detailed below, additional factors contribute).

3.3. Charge-Collection Lengths. Electrons generated near the back of the dye-coated electrode (for example, by illuminating the photoelectrode through the solution) obviously travel farther to reach the current collector than those supplied near the front of the electrode (for example, by illumination of the photoelectrode through the transparent conducting oxide support, for instance, the current collector). Thus, ratios of IPCE values for back-side versus front-side illumination report on the charge collection length within the film. Qualitatively, the more similar the two plots, the larger the photoelectrode's charge collection length.⁵³ For DSCs containing $Co(phen)_3^{3+/2+}$ as the redox species, the plots diverge greatly. The maximum IPCE values with this shuttle are 12% with front-side illumination and just 2% with back-side illumination (3% with TBP). For comparison, an otherwise similar I_3^-/I^- cell exhibited a maximum IPCE of 70% with

front-side illumination and 50% with back-side illumination (i.e., a ratio of 0.7).⁵⁴ The plots indicate that the charge collection length is (a) relatively short (Figure 3, top) when compared with I_3^-/I^- -containing DSCs (see Figure S1 of the Supporting Information), and (b) only marginally increased by adding *t*-butyl-pyridine.

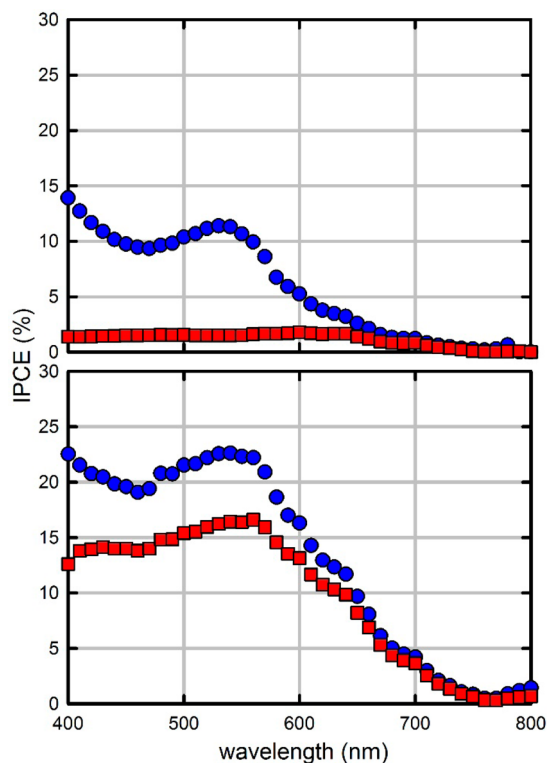


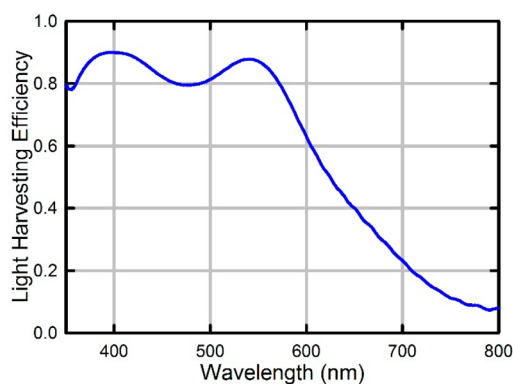
Figure 3. Front side (blue ●) and back side (red ■) IPCEs of $Co(phen)_3^{3+/2+}$ -containing DSCs. TBP (top) and Al_2O_3 -free DSCs. Al_2O_3 -coated photoanode (bottom); see Figure S1 of the Supporting Information for front- and back-side IPCEs of I_3^-/I^- .

Returning to DSCs employing $Co(phen)_3^{3+/2+}$ as the redox shuttle, we find that photoelectrode modification with ALD Al_2O_3 greatly enhances IPCE values. The maximum for front-side illumination increases from a peak of 12% to nearly 25%, while for back-side illumination the peak value increases from a meager 2% to 15% (Figure 3, bottom).⁵⁵ More importantly, in terms of effects of modifiers on charge-collection lengths, the ratio of IPCE maxima increases from ~ 0.17 to 0.6. Thus, ALD modification boosts the current output of DSCs that use $Co(phen)_3^{3+/2+}$ largely by boosting the photoelectrode's charge-collection length.

3.4. Overall Efficiencies. Overall energy conversion efficiencies for the various DSCs, calculated from fill-factors and the parameters discussed above, are summarized in Table 1. As noted above, to facilitate assessment of the effects, while avoiding complications from light scattering, nonoptimized cells were used [i.e., thin (6 μm) anodes, no scattering layer, and no $TiCl_4$ treatment]. On the basis of the light-harvesting efficiency data in Figure 4, the maximum photocurrent possible for anodes described herein is ca. 13 mA/cm^2 . The highest V_{OC} value obtained is 820 mV, which is comparable to the highest observed with champion or near-champion, N719-based cells.⁵⁶ The highest fill factor in Table 1 (albeit, for a different cell) is 0.74; the value is slightly below what has been reported for fully

Table 1. Summary of Photoelectrochemical Data for DSCs Containing Organic and/or Inorganic Surface Modifiers

	J_{SC} (mA/cm ²)	V_{OC} (mV)	FF	η (%)	$J_{interception}$ at V_{OC} (mA/cm ²)
I_3^-/I^-					
none	12.4	570	0.51	3.6	-3.7
TBP	11.2	730	0.58	4.7	-3.2
Al ₂ O ₃	8.1	700	0.64	3.6	-2.8
TBP and Al ₂ O ₃	5.5	820	0.70	3.1	-2.6
Co(phen) ₃ ^{3+/2+}					
none	1.4	490	0.68	0.46	-1.2
TBP	1.4	650	0.74	0.67	-1.0
Al ₂ O ₃	2.3	530	0.67	0.80	-1.6
TBP and Al ₂ O ₃	1.6	660	0.68	0.70	-0.84

**Figure 4.** Apparent light-harvesting efficiency for a 6 μm thick photoanode featuring a monolayer of adsorbed N719. The plot is uncorrected for light-scattering contributions in the corresponding optical extinction measurements and this accounts for the seemingly nonzero light-harvesting efficiency between 750 and 800 nm.

optimized, N719-based DSCs.⁵⁶ If these individually maximized parameters could be simultaneously expressed in a single cell, the highest efficiency we might expect for a N719-based DSC containing an interface-modified photoelectrode, simplified as described above, would be 7.4%. The highest efficiency found experimentally for our interface-modified cells is only 4.7% points, in particular, to the difficulty in enhancing charge collection length without sacrificing injection efficiency.

4. DISCUSSION

4.1. Triiodide/Iodide-Containing DSCs. The I_3^-/I^- redox couple is unparalleled for Ru-sensitized cells because devices incorporating this couple have electron collection lengths exceeding the thicknesses of typically employed photoanodes.⁵⁷ Thus, it is not surprising that the observed J_{SC} value for DSCs lacking modifiers (i.e., 12.4 mA/cm²) is nearly as great as the maximum value anticipated based on the light-harvesting efficiency. From the near agreement, we conclude that under the conditions of our experiments, the charge-injection efficiency is close to unity.

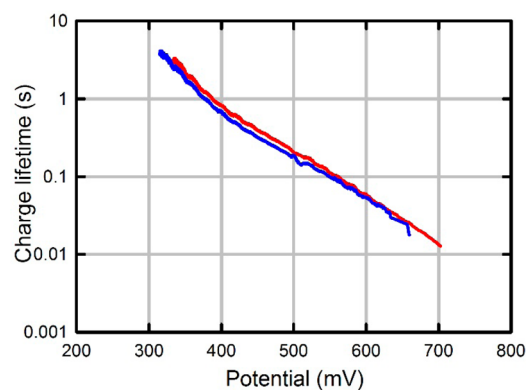
Electrode surface modification with TBP significantly decreases dark currents (suppresses $J_{interception}$), leading to the observed 160 mV increase in V_{OC} , in good agreement with previous work.²⁹ For J_{SC} , in contrast, the addition of TBP engenders a slight decrease. As noted above, charge-collection lengths are large for DSCs that use I_3^-/I^- , implying that at short-circuit, the charge-collection efficiency, η_{coll} , is close to

unity. Suppressing $J_{interception}$ (via TBP addition) can only improve η_{coll} and enhance J_{SC} .

Rather than enhancing η_{coll} , we believe that TBP lowers the short-circuit current density by decreasing the charge-injection yield, η_{inj} . The yield is determined by the kinetics of electron injection relative to the kinetics for competing dye-excited-state relaxation processes. The rate of electron injection is sensitive to the strength of the donor/acceptor (excited-dye/TiO₂ electrode) electronic coupling and to the ET driving force. The organic modifier is unlikely to influence electronic coupling significantly, but it could lower the driving force for injection by shifting E_{cb} to higher energy (more negative electrochemical potential). We have shown elsewhere, in studies with nonporous TiO₂ electrodes, that addition of TBP (or ALD alumina) shifts E_{cb} by, at most, a few tens of millivolts.⁵¹ While a shift of this magnitude is inconsequential in terms of direct effects on open-circuit photovoltages, it could be enough to slow the rate of electron injection by as much as 2-fold.⁵⁸ In turn, the injection yield for an otherwise optimized dye/semiconductor pair could drop by several percent or more.

The effects on J_{SC} and V_{OC} of electrode modification with alumina are similar to those arising from TBP addition, and we assume that the causes are similar. Previous work by Antilla et al.^{41,42} strongly supports the notion that even small amounts of ALD alumina can lower injection yields sufficiently to substantially degrade short-circuit current densities.⁵⁹

From eq 1, an alternative or additional explanation for the modifier-induced decreases in J_{SC} would be increases in $J_{recombination}$. This notion can be tested by comparing open-circuit photovoltage decays (OCPVD) with open-circuit voltage decays (OCVD; dark decays), since charge recombination can influence only the former. The observed close agreement of decay data for the two types of experiments (Figure 5) shows that for iodide-based cells, $J_{recombination}$ is not a significant contributor to J_{det} .⁶⁰

**Figure 5.** Comparison of open-circuit photovoltage decay (OCPVD) and open-circuit voltage decay (OCVD) measurements for DSCs containing I_3^-/I^- as the redox shuttle (no Al₂O₃ or TBP coatings). Blue: OCPVD; red: OCVD.

4.2. Co(phen)₃^{3+/2+}-Containing DSCs. J_{SC} values for Co(phen)₃^{3+/2+}-containing DSCs are smaller than those observed in I_3^-/I^- . As discussed above, for modifier-free DSCs the difference clearly is due to much less efficient charge collection when Co(phen)₃^{3+/2+} is the redox shuttle. From front-side/back-side IPCE measurements, the inorganic modifier significantly increases the charge-collection length, while the organic modifier has little effect on the collection

length (Figure 3; front-side/back-side illumination is nearly identical for TBP/TBP-free DSCs). Indeed, the charge-collection length with alumina-modified photoelectrodes approaches the thickness of the electrode itself. Nevertheless, J_{SC} reaches only about a quarter of the value anticipated for cells displaying both high injection yields and high charge-collection efficiencies. However, a different trend in current/voltage changes is observed; when TBP is used, only V_{OC} is significantly altered due to the suppression of $J_{interception}$ (Figure 2). Comparison of OCPVD and OCVD (Figure 6 and Figure

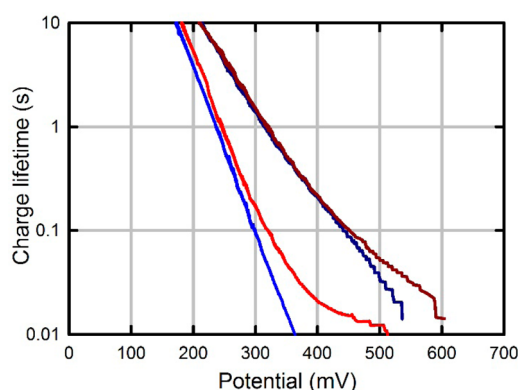


Figure 6. Comparison of open-circuit photovoltage decay (OCPVD) and open-circuit voltage decay (OCVD) measurements for DSCs containing $\text{Co}(\text{phen})_3^{3+/2+}$ as the redox shuttle. Blue: OCPVD; red: OCVD; dark blue: OCPVD with Al_2O_3 ; brown: OCVD with Al_2O_3 . See Figure S2 of the Supporting Information for TBP-containing OCPVD/OCVD plots.

S2 of the Supporting Information) illustrates that when Al_2O_3 is coated on the photoanode, the two plots look nearly identical, indicating that $J_{recombination}$ is not a significant contribution to J_{dark} (eq 2). However, when no Al_2O_3 is present then the two plots differ at high potentials, indicating that the oxidized dye is not being regenerated fast enough by $\text{Co}(\text{phen})_3^{2+}$, and thus there exists a significant contribution to J_{det} from $J_{recombination}$ (eq 2).

Since the modifiers act in distinctly different ways, it seemed possible that their combination might yield an additive advantage. Unfortunately, when both modifiers are used, J_{SC} decreases; the undesirable decrease in charge-injection yield more than offsets the beneficial effects of suppressing $J_{interception}$ and $J_{recombination}$.

5. CONCLUSIONS

The performance of dye-sensitized solar cells constructed with either $\text{Co}(\text{phen})_3^{3+/2+}$ or I_3^-/I^- as the redox shuttle and utilizing simplified photoanode structures (i.e., thin electrodes, no TiCl_4 treatment, no scattering layer) can be affected in a variety of ways, both favorable and unfavorable, by introduction of an organic surface-modifier (4-*tert*-butyl-pyridine), an inorganic surface-modifier (ALD-deposited Al_2O_3), or both. We find that for DSCs that are capable of quantitatively collecting photogenerated charges at short-circuit (i.e., those using I_3^-/I^-), added TBP boosts energy-conversion efficiencies by slowing electron interception and thereby increasing cell photovoltages. When surface modification instead consists of ALD Al_2O_3 or the combination of Al_2O_3 and TBP, photovoltages are again increased, but the gains are more than offset by decreases in photocurrent due to decreases in charge-

injection yield. The latter are traceable to small shifts in the conduction band-edge toward more negative electrode potential shifts that should decrease the thermodynamic driving force for dye injection.

For cells containing $\text{Co}(\text{phen})_3^{3+/2+}$ as the redox shuttle, charge collection is comparatively inefficient. Photoelectrode treatment with ALD alumina, either in isolation or in tandem with TBP, favorably influences cell efficiencies by increasing both J_{SC} and V_{OC} . The basis for increasing J_{SC} is mainly by suppressing losses due to electron recombination with the oxidized dye, with secondary contributions due to decreases in rates of interception of injected electrons by the oxidized form of the shuttle. Addition of TBP to a device both suppresses charge-interception and, at least with electrodes that are also ALD-modified, decreases the charge-injection yield. These opposing effects account for the inability of TBP to improve the overall efficiency in nonoptimized DSCs when alumina is already present. With I_3^-/I^- , ALD-alumina treatment boosts V_{OC} both by boosting J_{SC} and by suppressing dark current (i.e., slowing electron interception). In contrast, with $\text{Co}(\text{phen})_3^{3+/2+}$, ALD-alumina boosts V_{OC} by decreasing charge-recombination to the dye and thereby increasing J_{SC} . This interpretation is supported by OCVD versus OCPVD experiments. When $\text{Co}(\text{phen})_3^{3+/2+}$ is used, the combination of the two surface modifiers notably outperforms cells that contain only the organic modifier. In summary, surface modifiers influence not only rates of back electron transfer (both to the redox shuttle and the oxidized dye) but also rates of charge injection (more so for TBP than ALD alumina). Although TBP engenders slightly greater voltages in DSCs than does the inorganic modifier, the latter increases charge-collection lengths and enhances J_{SC} , sufficiently making it the preferred option when comparatively thick photoelectrodes are used in combination with cobalt-based redox shuttles.

■ ASSOCIATED CONTENT

📄 Supporting Information

Incident photon-to-current efficiency for iodide/triiodide-containing DSCs and open-circuit voltage/photovoltage decay of $\text{Co}(\text{phen})_3^{3+/2+}$ and TBP-containing DSCs. This material is available free of charge via the Internet at <http://pubs.acs.org>.

■ AUTHOR INFORMATION

Corresponding Author

*E-mail: j-hupp@northwestern.edu. Fax: +1-847-467-1425. Tel: +1-847-491-3504.

Author Contributions

The manuscript was written through contributions of all authors. All authors have given approval to the final version of the manuscript.

Notes

The authors declare no competing financial interest.

■ ACKNOWLEDGMENTS

J.T.H. gratefully acknowledges many enlightening discussions with both Marshal Newton and John Miller about electron-transfer phenomena and thanks them for sharing their extraordinary insights and for publishing their many groundbreaking findings. We gratefully acknowledge the ANSER Center, an Energy Frontier Research Center funded by the U.S. Department of Energy, Office of Science, Office of Basic Energy

Sciences under Award Number DE-SC0001059 for support of our work.

REFERENCES

- (1) Grätzel, M. Recent Advances in Sensitized Mesoscopic Solar. *Acc. Chem. Res.* **2009**, *42*, 1788–1798.
- (2) Yanagida, S.; Yu, Y.; Manseki, K. Iodine/Iodide-Free Dye-Sensitized Solar Cells. *Acc. Chem. Res.* **2009**, *42*, 1827–1838.
- (3) Nelson, J. *The Physics of Solar Cells*; Imperial College Press: London, U.K., 2006.
- (4) Kalyanasundaram, K. *Dye-Sensitized Solar Cells*; EPFL Press: Lausanne, 2010.
- (5) Yella, A.; Lee, H.-W.; Tsao, H. N.; Yi, C.; Chandiran, A. K.; Nazeeruddin, M. K.; Diau, E. W.-G.; Yeh, C.-Y.; Zakeeruddin, S. M.; Grätzel, M. Porphyrin-Sensitized Solar Cells with Cobalt (II/III)-Based Redox Electrolyte Exceed 12% Efficiency. *Science* **2011**, *334*, 629–634.
- (6) O'Regan, B.; Graetzel, M. A Low-Cost, High-Efficiency Solar Cell Based on Dye-Sensitized Colloidal Titanium Dioxide Films. *Nature* **1991**, *353*, 737–740.
- (7) Hagfeldt, A.; Boschloo, G.; Sun, L.; Kloo, L.; Pettersson, H. Dye-Sensitized Solar Cells. *Chem. Rev.* **2010**, *110*, 6595–6663.
- (8) Bomben, P.; Robson, K.; Koivisto, B. D.; Berlinguette, C. P. Cyclometalated Ruthenium Chromophores for the Dye-Sensitized Solar Cell. *Coord. Chem. Rev.* **2012**, *256*, 1438–1450.
- (9) Mishra, A.; Fischer, M. K. R.; Bäuerle, P. Metal-Free Organic Dyes for Dye-Sensitized Solar Cells: From Structure: Property Relationships to Design Rules. *Angew. Chem., Int. Ed.* **2009**, *48*, 2474–2499.
- (10) Martinson, A. B. F.; Hamann, T. W.; Pellin, M. J.; Hupp, J. T. New Architectures for Dye-Sensitized Solar Cells. *Chem.—Eur. J.* **2008**, *14*, 4458–4467.
- (11) Xie, Y.; Hamann, T. W. Fast Low-Spin Cobalt Complex Redox Shuttles for Dye-Sensitized Solar Cells. *J. Phys. Chem. Lett.* **2013**, *4*, 328–332.
- (12) Xu, D.; Zhang, H.; Chen, X.; Yan, F. Imidazolium Functionalized Cobalt Tris(Bipyridyl) Complex Redox Shuttles for High Efficiency Ionic Liquid Electrolyte Dye-Sensitized Solar Cells. *J. Mater. Chem. A* **2013**, *1*, 11933–11941.
- (13) Kashif, M. K.; Axelson, J. C.; Duffy, N. W.; Forsyth, C. M.; Chang, C. J.; Long, J. R.; Spiccia, L.; Bach, U. A New Direction in Dye-Sensitized Solar Cells Redox Mediator Development: In Situ Fine-Tuning of the Cobalt(II)/(III) Redox Potential through Lewis Base Interactions. *J. Am. Chem. Soc.* **2012**, *134*, 16646–16653.
- (14) Li, T. C.; Spokoynny, A. M.; She, C.; Farha, O. K.; Mirkin, C. A.; Marks, T. J.; Hupp, J. T. Ni(III)/(IV) Bis(Dicarbollide) as a Fast, Noncorrosive Redox Shuttle for Dye-Sensitized Solar Cells. *J. Am. Chem. Soc.* **2010**, *132*, 4580–4582.
- (15) Spokoynny, A. M.; Li, T. C.; Farha, O. K.; Machan, C. W.; She, C.; Stern, C. L.; Marks, T. J.; Hupp, J. T.; Mirkin, C. A. Electronic Tuning of Nickel-Based Bis(Dicarbollide) Redox Shuttles in Dye-Sensitized Solar Cells. *Angew. Chem., Int. Ed.* **2010**, *49*, 5339–5343.
- (16) Hamann, T. W. The End of Iodide? Cobalt Complex Redox Shuttles in DSSCs. *Dalton Trans.* **2012**, *41*, 3111–3115.
- (17) Hamann, T. W.; Farha, O. K.; Hupp, J. T. Outer-Sphere Redox Couples as Shuttles in Dye-Sensitized Solar Cells. Performance Enhancement Based on Photoelectrode Modification Via Atomic Layer Deposition Outer-Sphere Redox Couples as Shuttles in Dye-Sensitized Solar Cells. Performance Enhancement. *J. Phys. Chem. C* **2008**, *112*, 19756–19764.
- (18) Son, H.-J.; Wang, X.; Prasittichai, C.; Jeong, N. C.; Aaltonen, T.; Gordon, R. G.; Hupp, J. T. Glass-Encapsulated Light Harvesters: More Efficient Dye-Sensitized Solar Cells by Deposition of Self-Aligned, Conformal, and Self-Limited Silica Layers. *J. Am. Chem. Soc.* **2012**, *134*, 9537–9540.
- (19) Prasittichai, C.; Hupp, J. T. Surface Modification of SnO₂ Photoelectrodes in Dye-Sensitized Solar Cells: Significant Improvements in Photovoltage Via Al₂O₃ Atomic Layer Deposition. *J. Phys. Chem. Lett.* **2010**, *1*, 1611–1615.
- (20) Wu, J.; Lan, Z.; Hao, S.; Li, P.; Lin, J.; Huang, M.; Fang, L.; Huang, Y. Progress on the Electrolytes for DSSCs. *Pure Appl. Chem.* **2008**, *80*, 2241–2258.
- (21) Snaith, H. J. Estimating the Maximum Attainable Efficiency in Dye-Sensitized Solar Cells. *Adv. Funct. Mater.* **2010**, *20*, 13–19.
- (22) Hamann, T. W.; Jensen, R. A.; Martinson, A. B. F.; Van Ryswyk, H.; Hupp, J. T. Advancing Beyond Current Generation Dye-Sensitized Solar Cells. *Energy Environ. Sci.* **2008**, *1*, 66–78.
- (23) For simplicity we ignore the possibility that slow electron transfer kinetics at the counter electrode limit the short-circuit current density.
- (24) For simplicity, we ignore the possibility that the forward current density at the photoelectrode is potential-dependent (for example, because of a potential-dependent attenuation of injection efficiency arising from filling of near-band-edge states at very high light intensity).
- (25) Listorti, A.; O'Regan, B.; Durrant, J. R. Electron Transfer Dynamics in Dye-Sensitized Solar Cells. *Chem. Mater.* **2011**, *23*, 3381–3399.
- (26) Schiffrmann, F.; Vandevondele, J.; Hutter, J.; Urakawa, A.; Wirz, R.; Baiker, A. An Atomistic Picture of the Regeneration Process in Dye Sensitized Solar Cells. *Proc. Natl. Acad. Sci. U.S.A.* **2010**, *107*, 4830–4833.
- (27) Haque, S. A.; Palomares, E.; Cho, B. M.; Green, A. N. M.; Hirata, N.; Klug, D. R.; Durrant, J. R. Charge Separation Versus Recombination in Dye-Sensitized Nanocrystalline Solar Cells: The Minimization of Kinetic Redundancy. *J. Am. Chem. Soc.* **2005**, *127*, 3456–3462.
- (28) Feldt, S. M.; Wang, G.; Boschloo, G.; Hagfeldt, A. Effects of Driving Forces for Recombination and Regeneration on the Photovoltaic Performance of Dye-Sensitized Solar Cells Using Cobalt Polypyridine Redox Couples. *J. Phys. Chem. C* **2011**, *115*, 21500–21507.
- (29) Nazeeruddin, M. K.; Kay, A.; Rodicio, I.; Humphry-Baker, R.; Müller, E.; Liska, P.; Vlachopoulos, N.; Grätzel, M. Conversion of Light to Electricity by Cis-X₂bis(2,2'-Bipyridyl-4,4'-Dicarboxylate)-Ruthenium(II) Charge-Transfer Sensitizers (X = Cl⁻, Br⁻, I⁻, CN⁻, and SCN⁻) on Nanocrystalline TiO₂ Electrodes. *J. Am. Chem. Soc.* **1993**, *115*, 6382–6390.
- (30) Yu, S.; Ahmadi, S.; Sun, C.; Palmgren, P.; Hennies, F.; Zuleta, M.; Göthelid, M. 4-Tert-Butyl Pyridine Bond Site and Band Bending on TiO₂ (110). *J. Phys. Chem. C* **2010**, *114*, 2315–2320.
- (31) Göthelid, M.; Yu, S.; Ahmadi, S.; Sun, C.; Zuleta, M. Structure-Dependent 4-Tert-Butyl Pyridine-Induced Band Bending at TiO₂ Surfaces. *Int. J. Photoenergy* **2011**, *2011*, 1–6.
- (32) Kim, J.-Y.; Kim, J. Y.; Lee, D.-K.; Kim, B.; Kim, H.; Ko, M. J. Importance of 4-Tert-Butylpyridine in Electrolyte for Dye-Sensitized Solar Cells Employing SnO₂ Electrode. *J. Phys. Chem. C* **2012**, *116*, 22759–22766.
- (33) Kusama, H.; Orita, H.; Sugihara, H. TiO₂ Band Shift by Nitrogen-Containing Heterocycles in Dye-Sensitized Solar Cells: A Periodic Density Functional Theory Study. *Langmuir* **2008**, *24*, 4411–4419.
- (34) Liberatore, M.; Burtone, L.; Brown, T. M.; Reale, A.; Di Carlo, A.; Decker, F.; Caramori, S.; Bignozzi, C. A. On the Effect of Al₂O₃ Blocking Layer on the Performance of Dye Solar Cells with Cobalt Based Electrolytes. *Appl. Phys. Lett.* **2009**, *94*, 173113.
- (35) Terranova, U.; Bowler, D. R. Coating TiO₂ Anatase by Amorphous Al₂O₃: Effects on Dyes Anchoring through Carboxyl Groups. *J. Phys. Chem. C* **2012**, *116*, 4408–4415.
- (36) Fan, S.-Q.; Geng, Y.; Kim, C.; Paik, S.; Ko, J. Correlating the Photovoltaic Performance of Alumina Modified Dye-Sensitized Solar Cells with the Properties of Metal-Free Organic Sensitizers. *Mater. Chem. Phys.* **2012**, *132*, 943–949.
- (37) Yu, H.; Xue, B.; Liu, P.; Qiu, J.; Wen, W.; Zhang, S.; Zhao, H. High-Performance Nanoporous TiO₂/La₂O₃ Hybrid Photoanode for Dye-Sensitized Solar Cells. *ACS Appl. Mater. Interfaces* **2012**, *4*, 1289–1294.

(38) Law, M.; Greene, L. E.; Radenovic, A.; Kuykendall, T.; Liphardt, J.; Yang, P. ZnO-Al₂O₃ and ZnO-TiO₂ Core-Shell Nanowire Dye-Sensitized Solar Cells. *J. Phys. Chem. B* **2006**, *110*, 22652–22663.

(39) Tak Kim, J.; Ho Kim, S. Surface Modification of TiO₂ Electrode by Various over-Layer Coatings and O₂ Plasma Treatment for Dye Sensitized Solar Cells. *Sol. Energy Mater. Sol. Cells* **2011**, *95*, 336–339.

(40) Chandiran, A. K.; Nazeeruddin, M. K.; Grätzel, M. The Role of Insulating Oxides in Blocking the Charge Carrier Recombination in Dye-Sensitized Solar Cells. *Adv. Funct. Mater.* **2013**, 1615–1623.

(41) Antila, L. J.; Heikkilä, M. J.; Aumanen, V.; Kemell, M.; Myllyperkiö, P.; Leskelä, M.; Korppi-Tommola, J. E. I. Suppression of Forward Electron Injection from Ru(dcbpy)₂(NCS)₂ to Nanocrystalline TiO₂ Film as a Result of an Interfacial Al₂O₃ Barrier Layer Prepared with Atomic Layer Deposition. *J. Phys. Chem. Lett.* **2010**, *1*, 536–539.

(42) Antila, L. J.; Heikkilä, M. J.; Mäkinen, V.; Humalämäki, N.; Laitinen, M.; Linko, V.; Jalkanen, P.; Toppari, J.; Aumanen, V.; Kemell, M.; Myllyperkiö, P.; Honkala, K.; Häkkinen, H.; Leskelä, M.; Korppi-Tommola, J. E. I. ALD Grown Aluminum Oxide Submonolayers in Dye-Sensitized Solar Cells: The Effect on Interfacial Electron Transfer and Performance. *J. Phys. Chem. C* **2011**, *115*, 16720–16729.

(43) Fabregat-Santiago, F.; García-Cañadas, J.; Palomares, E.; Clifford, J. N.; Haque, S. A.; Durrant, J. R.; Garcia-Belmonte, G.; Bisquert, J. The Origin of Slow Electron Recombination Processes in Dye-Sensitized Solar Cells with Alumina Barrier Coatings. *J. Appl. Phys.* **2004**, *96*, 6903–6907.

(44) Chandiran, A. K.; Tetreault, N.; Humphry-Baker, R.; Kessler, F.; Baranoff, E.; Yi, C.; Nazeeruddin, M. K.; Grätzel, M. Subnanometer Ga₂O₃ Tunneling Layer by Atomic Layer Deposition to Achieve 1.1 V Open-Circuit Potential in Dye-Sensitized Solar Cells. *Nano Lett.* **2012**, *12*, 3941–3947.

(45) Another approach has been to incorporate long chain alkanes on the periphery of the dye molecules, thereby preventing the close approach of the dye with the semiconductor. In comparison with TBP additives and Al₂O₃ coatings, this method will also decrease the rates of dye-regeneration which, depending on the solubility and electron-transfer rates of the redox shuttle, can lead to charge-recombination between the oxidized form of the dye and an electron in the semiconductor. For representative examples of dyes with long alkyl chains and their effect on DSCs containing cobalt redox shuttles, the following two references are recommended: (a) Mosconi, E.; Yum, J.-H.; Kessler, F.; Gómez García, C. J.; Zuccaccia, C.; Cinti, A.; Nazeeruddin, M. K.; Grätzel, M.; De Angelis, F. Cobalt Electrolyte/Dye Interactions in Dye-Sensitized Solar Cells: A Combined Computational and Experimental Study. *J. Am. Chem. Soc.* **2012**, *134*, 19438–19453. (b) Feldt, S. M.; Gibson, E. A.; Gabriellsson, E.; Sun, L.; Boschloo, G.; Hagfeldt, A. Design of Organic Dyes and Cobalt Polypyridine Redox Mediators for High-Efficiency Dye-Sensitized Solar Cells. *J. Am. Chem. Soc.* **2010**, *132*, 16714–16724.

(46) Nazeeruddin, M. K.; Kay, A.; Rodicio, I.; Humphry-Baker, R.; Müller, E.; Liska, P.; Vlachopoulos, N.; Grätzel, M. Conversion of Light to Electricity by SCN⁻ on Nanocrystalline TiO₂ Electrodes. *J. Am. Chem. Soc.* **1993**, *115*, 6382–6390.

(47) Prasittichai, C.; Hupp, J. T. Surface Modification of SnO₂ Photoelectrodes in Dye-Sensitized Solar Cells: Significant Improvements in Photovoltage Via Al₂O₃ Atomic Layer Deposition. *J. Phys. Chem. Lett.* **2010**, *1*, 1611–1615.

(48) Koops, S. E.; O'Regan, B. C.; Barnes, P. R. F.; Durrant, J. R. Parameters Influencing the Efficiency of Electron Injection in Dye-Sensitized Solar Cells. *J. Am. Chem. Soc.* **2009**, *131*, 4808–4818.

(49) Koh, T. M.; Nonomura, K.; Mathews, N.; Hagfeldt, A.; Grätzel, M.; Mhaisalkar, S. G.; Grimsdale, A. C. Influence of 4-Tert-Butylpyridine in DSCs with Co^{II/III} Redox Mediator. *J. Phys. Chem. C* **2013**, *117*, 15515–15522.

(50) Yang, X.; Zhang, S.; Zhang, K.; Liu, J.; Qin, C.; Chen, H.; Islam, A.; Han, L. Coordinated Shifts of Interfacial Energy Levels: Insight into Electron Injection in Highly Efficient Dye-Sensitized Solar Cells. *Energy Environ. Sci.* **2013**, *6*, 3637–3645.

(51) Katz, M. J.; Vermeer, M. J. D.; Farha, O. K.; Pellin, M. J.; Hupp, J. T. Effects of Adsorbed Pyridine Derivatives and Ultrathin Atomic-Layer-Deposited Alumina Coatings on the Conduction Band-Edge Energy of TiO₂ and on Redox-Shuttle-Derived Dark Currents. *Langmuir* **2013**, *29*, 806–814.

(52) At V_{oc}, the forward and reverse currents are equal. In a theoretical device, J_{dark} at V_{oc} and J_{sc} would be theoretically equal.

(53) Barnes, P. R. F.; Anderson, A. Y.; Koops, S. E.; Durrant, J. R.; O'Regan, B. C. Electron Injection Efficiency and Diffusion Length in Dye-Sensitized Solar Cells Derived from Incident Photon Conversion Efficiency Measurements. *J. Phys. Chem. C* **2009**, *113*, 1126–1136.

(54) While the departure of the ratio from unity suggests a charge-collection length that does not span the full electrode, we have not accounted for back-side losses due to competitive light absorption by the platinum-coated counter electrode and by triiodide in the solution beyond electrodes.

(55) On the basis of the similar difference in front-side/back-side IPCE differences in an I₃⁻/I⁻-containing DSC, the remaining front-side/back-side differences in Co(phen)₃^{3+/2+} are primarily due to competitive light absorption by the platinum counter electrode and the electrolyte solution.

(56) Nazeeruddin, M. K.; Baranoff, E.; Grätzel, M. Dye-Sensitized Solar Cells: A Brief Overview. *Sol. Energy* **2011**, *85*, 1172–1178.

(57) Bertoluzzi, L.; Ma, S. On the Methods of Calculation of the Charge Collection Efficiency of Dye Sensitized Solar Cells. *Phys. Chem. Chem. Phys.* **2013**, *15*, 4283–4285.

(58) Recall that for small changes in driving force for electron-transfer reactions in the Marcus normal region, theory promises exponential modulations of rates of electron transfer. In the low-driving-force limit, a ca. 120 meV change in reaction free-energy should engender a factor of 10 change in rate ET constant.

(59) Alumina-induced diminution of charge-injection yields could conceivably arise not only from changes in driving force but also from changes in dye/electrode electronic coupling.

(60) Open-circuit photovoltage decay reports on back-ET to both the oxidized dye and the oxidized shuttle, while open-circuit voltage decay report on back-ET to only the shuttle. A comparison of these two plots illustrates the effect of the oxidized dye on the electron survival times; similar plots indicate no significant contribution from the oxidized dye while differing plots (often at high voltages/early decay times) indicate that regeneration is insufficient and thus recombination becomes problematic.